ON THE MODE II TESTING OF CARBON-FIBRE POLYMER COMPOSITES

B.R.K. Blackman and J.G. Williams†

In this paper the contribution of friction to the mode II delamination toughness of fibre-reinforced laminates has been assessed. It is shown that the conventional analyses used for the determination of G_{IIC} i.e. the compliance method and the corrected beam theory method require correction for friction, and that both of these analysis methods over-state the value of G_{IIC}. It is shown also that the failure to include friction in the analysis results in a deviation between the values of G_{IIC} deduced via the experimental compliance method and the values deduced from corrected beam theory. It is shown that friction corrections are significant, and in the case of a tough matrix composite (APC-2) and a glass-fibre epoxy composite may actually lead to the value of G_{IIC} being equivalent to the value G_{IC}, the mode I fracture toughness.

INTRODUCTION

There has been much interest recently in the mode II delamination testing of fibre reinforced polymer composites. However, progress towards an International Standard for measuring the mode II delamination toughness, G_{IIC}, has been slow and there remain a number of critical issues which need to be resolved before any testing standard can gain International acceptance.

Firstly there is the issue of choice of test method. A recent round-robin co-ordinated by VAMAS (Versailles Agreement on Materials and Standards) compared three experimental methods across an International platform. Labs in Europe, USA and Japan performed mode II tests using the ELS (end-loaded split), ENF (end notched flexure) and SENF (stabilised end notched flexure) test geometries. More recently, another version of the ENF test using four point bending has been proposed and is currently being assessed in a second round-robin. The final decision on the test method will likely be determined on the grounds of crack stability, repeatability, reproducibility and ease of use. Secondly, there is the issue of specimen calibration. In the ELS test, for example, different values of G_{IIC} are typically deduced depending upon whether the experimental compliance method or corrected beam theory methods of analysis are employed. Friction in the mode II test will influence the calibration of the specimen and will lead to discrepancies in the values of G_{IIC} deduced via the experimental compliance method and the corrected beam theory method. Finally,

† The authors are both from the Department of Mechanical Engineering, Imperial College, Exhibition Road, London SW7 2BX. UK.

there is the issue of the mechanism of crack growth under mode II loading conditions in composites. In a recent review article by O'Brien (1) it was suggested that under mode II loading, the crack does not grow in a continuous manner as previously assumed, but grows via the formation and subsequent coalescence of microcracks ahead of the main crack tip. This mechanism creates a characteristic hackle pattern on the fracture surfaces which in turn causes a locking of the sliding surfaces. This stress induced matrix microcracking was recently analysed by Lee (2) and such a mechanism could explain the high degree of scatter noted in mode II test data and in mixed-mode test data where the loading is predominantly mode II.

In the present paper, the role of friction in the mode II ELS test is investigated. An analysis based upon the assumption of a uniform shear stress acting on the cracked surfaces is presented and results for this case are given. A second analysis is also considered for the assumption that the shear stress is not uniform, but reaches a sharp peak at the crack tip. It is also indicated how the ELS test may be modified to allow the form of the shear stress distribution to be determined.

FRICTION IN MODE II

Background

A number of studies have previously been reported on the influence of friction on the measured values of G_{IIC} in the mode II ENF test. Gillespie et al (3) included the contact problem into a two dimensional FE model of the ENF test, and found that the assumed friction reduced the beam compliance and G_{IIC} values by up to 1% and 5% respectively. In an experimental study using the ENF test, Davies (4) found that for thick specimens, the values of G_{IIC} measured from specimens without a PTFE film separator between the crack surfaces were 20% higher than when PTFE film separators were used. Thus, the additional friction had caused a 20% overestimation of the fracture toughness. In the following section, the effect of friction on the measured G_{IIC} values in the mode II ELS test will be considered.

Assumption of uniform shear stress

The mode II ELS test geometry is shown in Figure 1. The analysis derived previously by Williams (5) for this mode II test ignores the frictional stresses acting on the crack faces. If we now include shear stress in our analysis and assume that it is uniform along the crack length, i.e. $\tau = \tau_o$, then the displacement of the beam shown in Figure 1 is given by:

$$\mathbf{u}_o = \frac{3}{2\mathbf{Ebh}^3}\left[\mathbf{P}\left(\frac{\mathbf{L}^3}{3}+\mathbf{a}^3\right)-\frac{4}{3}\tau_o\mathbf{bh.a}^3\right] \qquad \text{.....................(1)}$$

Where E is the axial modulus of the beam. If we now define a parameter α which is the ratio of the frictional shear stress to the applied shear stress or:

$$\alpha = \frac{\tau_o}{\hat{\tau}} \qquad \text{...(2)}$$

Then it can be easily shown that for the ELS test:

$$\alpha = \frac{4}{3}\frac{\tau_o \mathbf{bh}}{\mathbf{P}} \qquad \text{..(3)}$$

Then the compliance of the beam may be written as:

$$C = \frac{u_o}{P} = \frac{3a^3}{2Ebh^3}(1-\alpha) + \frac{L^3}{2Ebh^3} \quad \text{.................................(4)}$$

Therefore, including this frictional term we can write:

$$G_{IIc} = \frac{P^2}{2B}\frac{dC}{da} = \frac{9P^2a^2(1-\alpha)}{4Eb^2h^3} \quad \text{.................................(5)}$$

And noting that when we do not consider friction, the value of G_{IIC} deduced via beam theory (BT) is:

$$G_{IIc}(BT) = \frac{9P^2a^2}{4Eb^2h^3} \quad \text{...(6)}$$

It is noted that equation (5) is equivalent to the value of G_{IIC} which is determined from the compliance method of analysis, because the frictional shear stress, τ_o, influences the calibration of the test, i.e. the plot of C versus a^3 from the ELS test will yield a gradient, m, which has been altered by friction. Hence we can describe the value of G_{IIC} determined from equation (6) as G_{IIC} (BT) and the value determined from equation (5) as that obtained from the elastic compliance method of analysis or G_{IIC} (ECM). However, it can be shown that the exact solution for G_{IIC}, obtained by considering the shear stress contribution to the bending moment at the crack tip, is given by:

$$G_{IIc}(TRUE) = \frac{9P^2a^2}{4Eb^2h^3}(1-\alpha)^2 \quad \text{.................................(7)}$$

Therefore, in the ELS test, both beam theory and the elastic compliance method will overstate the value of G_{IIC}, but by differing amounts. Beam theory yields the higher value and the exact solution yields the lower value. They are related via equation 8:

$$\frac{\{G_{IIC}(ECM)\}^2}{G_{IIC}(BT)} = G_{IIC}(TRUE) \quad \text{.................................(8)}$$

As usual, equations (5) to (7) require correction for shear deflection and rotation of the crack tip and this may be achieved by adding a term Δ_{II} to the crack length. The results presented later are corrected in this way, i.e. G_{IIC} (BT) is the corrected beam theory.

<u>Assumption of non-uniform shear stress</u>

The analysis above assumed that the frictional shear stress, τ_o, was uniform along the entire crack length. In practice, the shear stress distribution probably has a more complicated form. If we now assume a shear stress distribution of the form:

$$\tau = \tau_o\left(\frac{x}{a}\right)^n \quad \text{...(9)}$$

Then we can proceed as before and write the exact solution for G_{IIC} as:

$$G_{IIC} = \frac{9P^2a^2}{4Eb^2h^3}(1-\alpha)\left[1-\frac{2\alpha}{(1+n)(2+n)}\right] \qquad \text{..................(10)}$$

The dependence of the shear stress distribution upon the parameter n is shown in Figure 2. When n=0, we revert to the uniform shear stress assumption above. A high n gives a sharp peak to the shear stress at the crack tip. One possible method to determine n and α would be to measure both the vertical displacement u_o and also the horizontal sliding displacement between the lower and upper beam. In the present work however, the assumption of a uniform shear stress will be made.

EXPERIMENTAL

Procedure for uniform shear stress

The parameter α can be deduced from the ELS test and the experimental procedure is described in an ESIS protocol (6). The parameter can be deduced by comparison of the values of G_{IIC} determined via beam theory and via the elastic compliance method, as will be shown later. The values of the crack length require correction by the addition of Δ_{II} as specified in (6). The materials tested contained folded PTFE insert films up to the initial crack length, a_o.

Results assuming a uniform shear stress distribution

The parameter α and the corrected value of G_{IIC}, termed G_{IIC} (TRUE), was deduced by comparison of the two data reductions methods, namely the elastic compliance method and beam theory, i.e. by equations (7) and (8). Test data which had previously been obtained from tests on: (i) a carbon-fibre epoxy composite, (ii) a carbon-fibre PEEK (APC-2) composite and for comparison (iii) a glass-fibre epoxy composite were reanalysed and typical results are shown in Table 1.

TABLE 1- Values of α and G_{IC}, G_{IIC} (BT), G_{IIC} (ECM) and corrected G_{IIC} i.e. G_{IIC} (TRUE) for three materials tested using the ELS configuration.

			(J/m^2)		
Material	α	G_{IC}	G_{IIC} (BT)	G_{IIC} (ECM)	G_{IIC}(TRUE)
CF epoxy	0.12	150	560	493	434
APC-2	0.09	2000	2500	2275	2070
GF epoxy	0.39	1000	4000	2440	1488

The value of the parameter α obtained for each material is tabulated. The value of G_{IC} measured from a mode I DCB test is shown and the values of G_{IIC} (BT) i.e. G_{IIC} from corrected beam theory and G_{IIC} (ECM) are shown. The final column shows the 'TRUE' or corrected value of G_{IIC} with the friction term included i.e. from equation (8). It can be seen that: G_{IIC} (BT)>G_{IIC} (ECM)>G_{IIC}(TRUE).

From the above results it is of interest to compare the values of corrected or true G_{IIC} with the values of G_{IC}. The rationale for doing this is that if G_{IIC} was simply 'G_{IC} plus friction' then the values of G_{IIC} (TRUE) would be equal to the values of G_{IC}. The results in Table 1 indicate that for the APC-2 composite, an α of 0.09 is almost enough to reduce G_{IIC} to G_{IC}. This is shown in Figure 3 which displays R-curve data for the APC-2 composite and it is seen that the value of G_{IIC} (TRUE) is only 3-4% higher than the value of G_{IC}. Also, for the glass-fibre epoxy composite, an α of 0.39 is again sufficient to reduce G_{IIC} to G_{IC}. However, for the carbon-fibre epoxy composite, an α of 0.12 is clearly insufficient to reduce G_{IIC} to G_{IC}. These results therefore show that for the APC-2 composite and the glass-fibre epoxy composite, then friction alone may account for the difference between G_{IIC} and G_{IC}. However, in the carbon-fibre epoxy composite, there must be another mechanism occurring which causes G_{IIC} to be very much greater than G_{IC}. Other studies have shown that this is mechanism is probably microcracking, i.e. microcracks forming ahead of the main crack which then coalesce to leave the characteristic hackle pattern on the fracture surface.

CONCLUSIONS

The contribution of friction to the values of the mode II fracture toughness, G_{IIC} has been derived by assuming firstly a uniform friction shear stress acting on the crack surfaces and then secondly by assuming a more complex shear stress distribution, with the stress rising to a sharp peak at the crack tip. By applying the first case, i.e. of uniform shear stress, the friction contribution to mode II test data obtained from the end-loaded split test has been assessed for three different composite materials. The amount of friction deduced from this analysis was significant when related the values of G_{IIC}. Indeed, when the values of G_{IIC} obtained from beam theory were corrected for this friction component, then values very close to G_{IC} were obtained for the APC-2 composite and a glass-fibre epoxy composite. However, for one case (a carbon-fibre epoxy composite) the friction component was insufficient to correct G_{IIC} down to G_{IC}, so in this case another mechanism may also be operating in mode II to cause G_{IIC} to be very much greater than G_{IC}. The application of the second case, i.e. with a non-uniform shear stress acting on the crack surfaces may be investigated by performing a modified ELS test in which both the vertical beam displacement and the horizontal sliding beam displacement are measured. Experimental work investigating this modified procedure is at an early stage.

REFERENCES

(1) O'Brien T.K., "Composite Interlaminar Shear Fracture Toughness, G_{IIC}: Shear Measurement or Sheer Myth?" NASA Technical Memorandum, 1997, number 110280, report 1312.

(2) Lee S.M., "Mode II delamination failure mechanisms of polymer matrix composites." J. Mat Sci. 32, 1997, pp. 1287-1295.

(3) Gillespie J.R., Carlsson L.A., and Pipes R.B. "Finite element analysis of the ENF specimen for measuring mode II fracture toughness." Composites Sci. & Tech. 27 , 1986, pp. 177-197.

(4) Davies P. "Influence of ENF specimen geometry and friction on the mode II delamination resistance of Carbon/PEEK." J. of Thermoplastic Composite Materials 10, 1997, pp. 353-361.

(5) Hashimi S., Kinloch A.J., and Williams J.G., "The analysis of interlaminar fracture in uniaxial fibre-polymer composites" Proc. R. Soc. Lond. A 427, 1990, pp. 173-199.

(6) ESIS protocol "Determination of the Mode II delamination resistance of unidirectional fibre-reinforced polymer laminates using the end-loaded split specimen." Version 95-11-10.

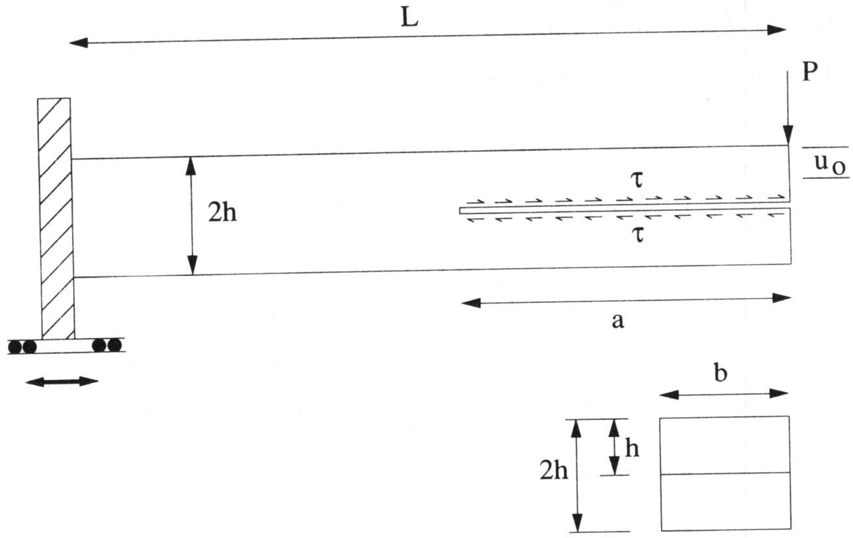

Figure 1 End-loaded split (ELS) mode II test arrangement

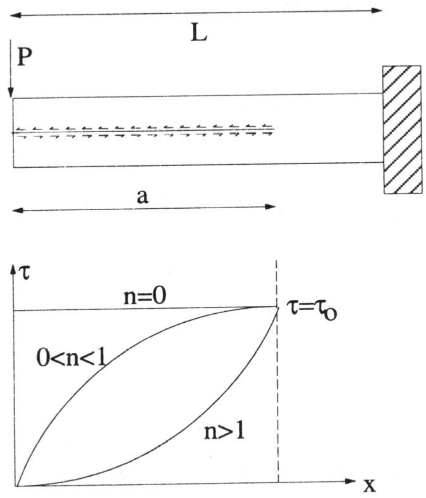

Figure 2 Possible forms of the shear stress distribution

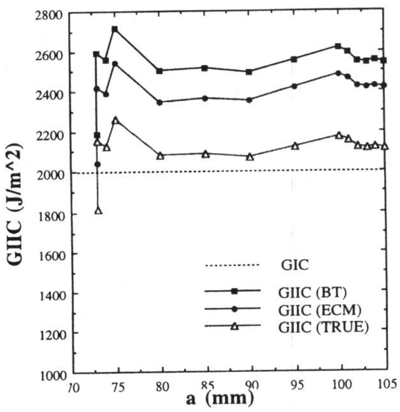

Figure 3 G_{IIC} vs crack length for the APC-2 composite